ResearchGate

See discussions, stats, and author profiles for this publication at: https://www.researchgate.net/publication/12771815

Probing Intramolecular Orientations in Rhodopsin and Metarhodopsin II by Polarized Infrared Difference Spectroscopy †

ARTICLE *in* BIOCHEMISTRY · NOVEMBER 1999

Impact Factor: 3.02 · DOI: 10.1021/bi9909501 · Source: PubMed

CITATIONS
13

READS
19

5 AUTHORS, INCLUDING:

Kenneth J Rothschild
Boston University
188 PUBLICATIONS **6,817** CITATIONS
SEE PROFILE

Willem J Degrip
Radboud University Nijmegen
262 PUBLICATIONS **7,213** CITATIONS
SEE PROFILE

Available from: Willem J Degrip
Retrieved on: 30 January 2016

Probing Intramolecular Orientations in Rhodopsin and Metarhodopsin II by Polarized Infrared Difference Spectroscopy†

Frank DeLange,‡ Petra H. M. Bovee-Geurts,‡ Arthur M. A. Pistorius,‡ Kenneth J. Rothschild,§ and Willem J. DeGrip*,‡

Department of Biochemistry, FMW-160, Institute of Cellular Signalling, University of Nijmegen, P.O. Box 9101, 6500 HB Nijmegen, The Netherlands, and Department of Physics and Molecular Biophysics Laboratory, Boston University, Boston, Massachusetts 02215

Received April 26, 1999; Revised Manuscript Received July 14, 1999

ABSTRACT: The light-induced conformational changes of rhodopsin, which lead to the formation of the G-protein activating metarhodopsin II intermediate, are studied by polarized attenuated total reflectance infrared difference spectroscopy. Orientations of protein groups as well as the retinylidene chromophore were calculated from the linear dichroism of infrared difference bands. These bands correspond to changes in the vibrational modes of individual molecular groups that are structurally active during receptor activation, i.e., during the rhodopsin to metarhodopsin II transition. The orientation of the transition dipole moments of bands previously assigned to the carboxyl (C═O) groups of Asp83 and Glu113 has been determined. The orientation of specific groups in the retinylidene chromophore has been inferred from the dichroism of the bands associated with the polyene C−C, C═C, and hydrogen-out-of-plane vibrations. Interestingly, the use of polarized infrared light reveals several difference bands in the rhodopsin to metarhodopsin II difference spectrum which were previously undetected, e.g., at 1736 and 939 cm^{-1}. The latter is tentatively assigned to the hydrogen-out-of-plane mode of the $HC_{11}═C_{12}H$ segment of the chromophore. Our data suggest a significant change in orientation of this group in the late phase of rhodopsin activation. On the basis of available site-directed mutagenesis data, bands at 1406, 1583, and 1736 cm^{-1} are tentatively assigned to Glu134. The main features in the amide regions in the dichroic difference spectrum are discussed in terms of a slight reorientation of helical segments upon receptor activation.

Rhodopsin, the vertebrate visual pigment responsible for scotopic vision, is located in the retinal rod cells. It is a 7-helix integral membrane protein and is considered to be a paradigm for the vast superfamily of G-protein coupled receptors (GPCRs)[1] (*1*). It is generally assumed that the 7-helix bundle is arranged such that a cleft is formed in the interior part of the protein which accommodates the light sensitive ligand (and chromophore) 11-*cis*-retinal, covalently bound through a Schiff base linkage to a lysine in helix 7. Photoexcitation of rhodopsin is triggered by ultrafast (<200 fs) (*2*) 11-cis → all-trans photoisomerization of the chromophore, which subsequently initiates a series of thermal conformational transitions in the protein (bathorhodopsin ↔ blue-shifted intermediate → lumirhodopsin → metarhodopsin I ↔ metarhodopsin II) (*3, 4*). At physiological temperature, metarhodopsin II, the active state of the receptor (*5, 6*), is formed within milliseconds after isomerization of the chromophore. Since activation of a GPCR is assumed to require protein conformational changes, understanding the molecular events underlying rhodopsin activation is not only extremely important for understanding the first step in vision but also is likely to hold significance for other GPCRs as well.

Fourier transform infrared (FTIR) difference spectroscopy has been extensively used to study the structural changes occurring in the photoreceptor membrane upon light activation. With this technique, conformational changes in the chromophore, peptide backbone, lipid matrix, and bound H_2O, as well as changes in protonation state and/or hydrogen-bonding environment of Asp, Glu, Cys, and Tyr residues have been detected at the various stages of rhodopsin activation (*7*−*24*). Assignment of vibrational bands to individual protein groups has been accomplished in combination with site-directed mutagenesis (*14*, *16*, *23*) and recently also by stable-isotope labeling of the protein (*24*).

Here, we describe the use of polarized attenuated total reflectance (ATR) FTIR difference spectroscopy to investigate the structural changes of bovine rhodopsin as it undergoes the transition from the dark-state to the active (metarhodopsin II) conformation. This method combines the sensitivity of infrared spectroscopy with the ability of polarized spectroscopy to probe the orientation relative to the membrane plane of the transition dipole moment associated with specific bands. This approach is complementary to earlier polarized FTIR studies of the absolute absorption

† This work was supported by grants from the Council for Chemical Research of The Netherlands Organization for Scientific Research (CW-NWO, WG 330-011) to W.D.G.

* To whom correspondence should be addressed. Fax: +31-243540525. Phone: +31-243614263. E-mail: wdegrip@baserv.uci.kun.nl.

‡ University of Nijmegen.

§ Boston University.

[1] Abbreviations: ATR, attenuated total reflectance; FTIR, Fourier transform infrared; GPCR, G-protein coupled receptor; HOOP, hydrogen-out-of-plane; IR, infrared; LD, linear dichroism; TDM, transition dipole moment; ROS, rhodopsin in native disk membranes isolated from bovine rod outer segments.

10.1021/bi9909501 CCC: $18.00 © xxxx American Chemical Society
Published on Web 00/00/0000 PAGE EST: 9.2

which revealed information about the orientation of structural components of the protein, e.g., α-helices, relative to the membrane plane (*25, 26*). In the case of difference spectroscopy, however, information is obtained about the relative orientation of specific structurally active molecular groups including previously assigned protein residues and retinylidene groups (or vibrational modes). Our data also complement the results obtained using other experimental approaches which probe orientation of structural components of rhodopsin, including the early visible dichroism studies (*27*−*29*) and, more recently, solid-state NMR studies (*30*). The macroscopic orientation of secondary structure elements we calculate basically agrees with earlier transmission FTIR studies on bovine rhodopsin (*26*). Our polarized difference spectra clearly reveal several new, previously unobserved bands throughout the entire spectral range (4000−800 cm^{-1}). The dominant features in the amide regions suggest that there occurs a small reorientation of helical segments in the activation step of rhodopsin. A novel band at 939 cm^{-1}, assignable to a HOOP mode in metarhodopsin II, is considered to reflect a reorientation of the retinal HC_{11}═$C_{12}H$ group in the metarhodopsin I to metarhodopsin II transition. Bands at 1406, 1583, and a previously undetected band near 1736 cm^{-1} are tentatively assigned to the symmetric and asymmetric carboxylate and carbonyl stretching vibrations of Glu134, which was proposed to protonate upon formation of metarhodopsin II (*31*).

MATERIALS AND METHODS

Preparation of Rhodopsin. ROS was prepared as previously described (*32*). The A_{280}/A_{500} typically was between 1.9 and 2.1. Membrane suspensions in doubly distilled water (typically 130 nmol/mL in rhodopsin) were stored in an argon atmosphere at −80 °C until further use. All manipulations involving rhodopsin were performed under dim red light (RG645 cutoff filter, Schott). Throughout the experiments, a Mes H_2O/D_2O buffer (40 mM Mes, 260 mM NaCl, 10 mM KCl, 4 mM $CaCl_2$, and 0.2 mM EDTA, pH/pD 6) was used.

ATR-FTIR Measurements. Samples were prepared by slowly drying 30 μL of ROS suspension (about 4 nmol of rhodopsin) under a gentle stream of nitrogen onto a 50 × 20 × 2 mm^3 (l × w × h) Ge internal reflection element (EJ3121, Harrick Scientific Corporation, Ossining, NY). Hereafter, the Ge element was placed in a vacuum desiccator for 15 min to remove residual water. Subsequently, the sample was mounted into a modified, temperature controlled, variable angle ATR unit (MEC-1W in combination with TMP-V, Harrick) and polarized dark spectra were recorded at ambient temperature. For the analysis of the rhodopsin to metarhodopsin II transition, the membranes were humidified with either H_2O or D_2O buffer. Deuteration of the sample was accomplished by putting 50 μL of D_2O on top of the dried sample, now placed in a nitrogen purged glovebag. The sample was left to exchange for 2−3 h. After this period, the sample was redried before mounting it into the ATR cell, to allow a well-defined humidification with D_2O buffer. Six microliters of D_2O buffer was then placed on top of the sample and, in total, 50 μL of D_2O buffer on the inside of the sample cell's covering lid. Data collection typically started 6 h after sealing the cell. Thus, the samples had been in contact with bulk D_2O for at least 8 h prior to data collection. Spectra were recorded at 10 °C, since under these conditions metarhodopsin II is sufficiently stable [$t_{1/2}$ = 30 min (*17*), after data acquisition (see below) 70% metarhodopsin II still remains]. Sample humidification with H_2O buffer, and all subsequent procedures were performed under identical conditions as humidification with D_2O.

Polarized ATR-FTIR spectra were recorded using a wire-grid BaF_2 polarizer (Graseby Specac, Kent, U.K.) placed in the IR beam of a Mattson Cygnus 100 FTIR spectrometer (Mattson, Madison, WI) equipped with a narrow band Hg-Cd-Te detector. Spectra were derived from 256 single beam scans (1 min aquisition time), taken at 8 cm^{-1} resolution. Interferograms were doubly zero-filled and apodized using a triangular function, prior to further processing. The polarized single beam spectra were ratioed against a correspondingly polarized background. The orientation of the polarizer could be controlled with the spectrometer computer, and spectra were recorded with the polarization of the IR probe beam alternately parallel (||) and perpendicular (⊥) to the plane of incidence. In this way, we were able to signal average the parallel and perpendicular data sets in the bleaching experiments over the same time span.

Photoactivation of the samples was accomplished by illumination with yellow light (40 s) using a 20 W halogen lamp equipped with a KG1 heat filter and an OG530 cutoff filter (both filters from Schott). Difference spectra (metarhodopsin II minus rhodopsin) were computed by subtracting the average of at least eight spectra, recorded with the same polarization of the IR probe beam (at least 2048 co-added interferograms), taken before and after illumination, respectively.

Dichroic difference (LD) spectra were calculated by subtracting (difference) absorption spectra of the sample taken with perpendicularly polarized light (⊥) from those taken with parallel polarized light (||) using the scaling factor c: $LD = || - c \times \perp$. The factor c was determined interactively from the absolute absorption data in the dried or humidified state, by optimizing the sign and relative magnitude of the dichroic difference bands corresponding to the lipid methyl and methylene CH stretching modes, i.e., the ν_s (CH_3) band at 2875 cm^{-1} and the ν_{as} and ν_s (CH_2) bands at 2924 and 2853 cm^{-1}, respectively. Since the CH_2 vibrations are known to have their average transition moments perpendicular to the acyl chain long axis, i.e., perpendicular to the plane of incidence, in oriented fluid bilayers, their respective LD signals are expected to be overall negative. The reverse holds for the CH_3 symmetric stretching mode since its transition moment lies approximately parallel to the lipid acyl chains, and in oriented samples this band should give rise to positive LD (*33*). For presentation purposes, the same scaling was used to calculate the LD of the absolute absorbance spectra (in the dried and humidified state) as well as that of the light-induced difference spectra of the sample. We emphasize, however, that the LD spectra were used only for visualization purposes; the actual calculations of the linear dichroism of specific bands were based on the original, unscaled data.

Calculation of Orientations from ATR-FTIR Dichroism. The method applied here to determine the angle between the dipole moment of a specific vibrational mode corresponding to a dichroic band and the normal of the ATR internal reflection element is essentially similar to that

previously described (*34*−*37*). Briefly, a dichroic ratio, R_{ATR}, is defined as

$$R_{ATR} = \int A_{||}(\nu)\, d\nu / \int A_{\perp}(\nu)\, d\nu \quad (1)$$

where $\int A_{||,\perp}(\nu)\, d\nu$ are the integrated intensities of a certain vibrational band in the frequency range $d\nu$. From the dichroic ratio, and an estimation of the electric field amplitudes of the evanescent wave at the surface of the internal reflectance element (E_x, E_y, and E_z; *xy*-plane parallel to the surface of the Ge element), an order parameter *S* is calculated for the orientation of the structural element (*38*):

$$S = 2(E_x^2 - R_{ATR}E_y^2 + E_z^2)/ [(3\cos^2\alpha - 1)(E_x^2 - R_{ATR}E_y^2 - 2E_z^2)] \quad (2)$$

The average angle, θ, between the main axis of symmetry of the structural element and the membrane normal, relates to *S* through the expression

$$S = 3/2\,\langle\cos^2\theta\rangle - 1/2 \quad (3)$$

The order parameter is a time- and space-averaged function of θ, which is symbolized with the brackets in eq 3. In eq 2, a scaling factor $1/S_\alpha = 2/(3\cos^2\alpha - 1)$ has been introduced to account for the angle α between the transition dipole moment of the vibration and the main axis of symmetry of the structural element. Similar correction factors can be introduced to account for membrane disorder (S_m) and imperfect surface flatness (S_f) of the ATR crystal. However, here we take $S_m = S_f = 1$, i.e., basically a perfectly flat ATR surface and a perfectly oriented membrane multilayer is assumed. Note that due to this assumption we probably slightly underestimate the degree of orientation of the photoreceptor membrane segments (see results).

Electric field amplitudes were estimated based on the semi-infinite-bulk (or two-phase) approximation. In the case of unit incoming amplitude for both polarizations, the electric field amplitudes in the *x*, *y*, and *z* direction (eq 2) are given by (*39*)

$$E_x = 2(\sin^2\phi - n_{31}^2)^{1/2}\cos\phi / [(1 - n_{31}^2)^{1/2}[(1 + n_{31}^2)\sin^2\phi - n_{31}^2]^{1/2}] \quad (4a)$$

$$E_y = 2\cos\phi/(1 - n_{31}^2)^{1/2} \quad (4b)$$

$$E_z = 2\sin\phi\cos\phi / [(1 - n_{31}^2)^{1/2}[(1 + n_{31}^2)\sin^2\phi - n_{31}^2]^{1/2}] \quad (4c)$$

Here, ϕ is the angle of incidence between the IR beam and the Ge element (set to 45°), and n_{31} ($= n_3/n_1$) is the ratio between the refractive indices of the sample ($n_3 = 1.7$) (*26*) and the Ge crystal ($n_1 = 4$). Thus, throughout this work, we used $E_x = 1.38$, $E_y = 1.56$, and $E_z = 1.73$. The use of eq 4, specifically applying to the semi-infinite bulk case, is based on the assumption that the thickness of the sample [typically in the order of 10−20 μm (*34*)] is much larger than the penetration depth of the evanescent wave [about 1.4−2 μm in the spectral range 2000−1000 cm^{-1} (*35*)].

Data Analysis. All spectral analyses were performed using the GRAMS/32 Spectral Notebase program suite (Galactic Industries, Nashua, NH). Dichroic ratios were determined from peak heights as well as from the integrated intensities of the bands in the absolute absorbance spectra. Either baselines were calculated between data points limiting the integrating intervals or a global (straight line) baseline correction was performed by zeroing the 3800, 2600, 1900, and 945 cm^{-1} data points. In addition, in the case of the amide I region, curve-fitting analyses were performed in order to resolve the relative contribution of the α-helices to this band. For this, spectra were baseline corrected in the region 1900−945 cm^{-1}, and a maximum of 13 bands was used to curve-fit the 1790−1415 cm^{-1} region (*40*). The dichroic ratios corresponding to the α-helical structures were determined from the integrated intensity of the band centered at 1655 cm^{-1}. For the analysis of the rhodopsin → metarhodopsin II difference spectra, dichroic ratios were determined from the integrated intensities of the difference bands. Integrating intervals were chosen such that only one dichroic difference band fell in that region, thus minimizing interference from overlapping bands. Throughout this work, the average or apparent tilt angle θ is calculated from eq 3 by equating $\langle\cos^2\theta\rangle = \cos^2\langle\theta\rangle$, i.e., by assuming an infinitely narrow distribution of TDM orientations contributing to the absorption band under study.

RESULTS

Figure 1 compares the linear dichroism (LD) of an oriented ROS membrane film in darkness in the dried (Figure 1a) and humidified state (Figure 1b). The sample presented in Figure 1b was also used for the photoactivation experiments, presented in Figures 2 and 3. Panels b1 and b2 derive from the same sample as shown in Figure 1a; and the same scaling factor ($c = 1.70$) was used to calculate the LD spectrum in the humidified state (LD = || − 1.70 × ⊥). Panels b3 and b4 show the absorbance data from a sample in D_2O ($c = 1.54$). In all cases, the LD spectra are dominated by the positive (+) amide A (3287 cm^{-1}) and amide I (1654 cm^{-1}) contributions and negative (−) amide II (1545 cm^{-1}) contribution, typical for a net transmembrane orientation of α-helical structures (*26*, *37*, *41*−*43*). Moreover, LD signals from the lipid moiety are observed at 1740 (−), 1219 (−), and 1060 cm^{-1} (+). The latter bands are assigned to the phospholipid ester carbonyl stretch and the antisymmetric and symmetric PO_2^- double bond stretch, respectively, and their relative dichroism is in agreement with previously published data on oriented phospholipid containing membranes (*33*, *34*, *44*). Clearly, the qualitative orientation of the dried membrane film is well preserved upon humidification with H_2O/D_2O buffer.

Hydrogen−*Deuterium Exchange.* As previously shown, the FTIR-ATR spectra of ROS in D_2O exhibit a characteristic downshift of the amide II band from 1545 to near 1450 cm^{-1} (amide II′) (*45*). The amide II mode is assigned to (primarily) N−H bending vibrations of peptide amide groups (*46*), therefore, the isotope induced shift of this band provides a measure of the fraction of peptide groups undergoing hydrogen−deuterium (H/D) exchange. The relative amount of peptides undergoing H/D exchange was estimated by comparing the ratio of the (residual) amide II band intensity to the amide I band intensity in D_2O, w_D, to that before H/D exchange in a dehydrated sample, w_H. Integrating intervals ranged 1710−1587 cm^{-1} and 1580−1520 cm^{-1} for the amide

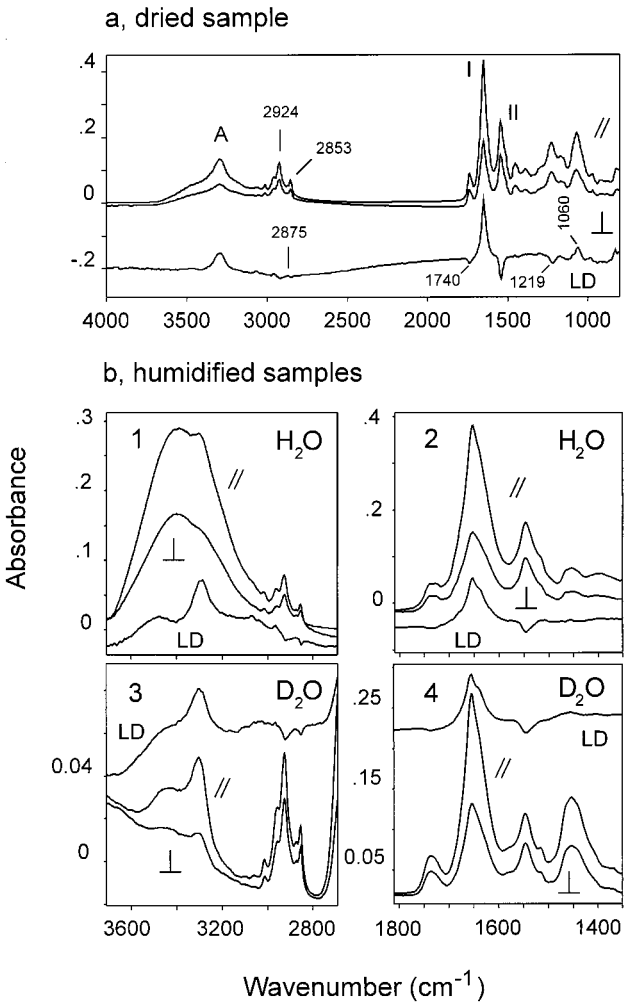

FIGURE 1: FTIR spectra of ROS membranes using either parallel (||) or perpendicular (⊥) polarized IR light. (a) Dried ROS membranes, (b1−b4) humidified ROS membranes: (b1 and b2) ROS in H_2O buffer and (b3 and b4) ROS in D_2O buffer. Amide A, I and II bands are indicated in panel a. LD denotes the difference spectrum between || and ⊥, identifying dichroic bands (LD = || − $c \times \perp$), c factor (see text) was 1.70 in panels a, b1, and b2, and 1.54 in panels b3 and b4. Traces shown are the average of 1280 scans. Note the differences in the frequency scale between panels a and b and the different absorbance scales for all figures. In all panels, the absorbance scales are those corresponding to the ||-spectra. In panels a and b1, the LD signal has been scaled by a factor of 2 for better comparison.

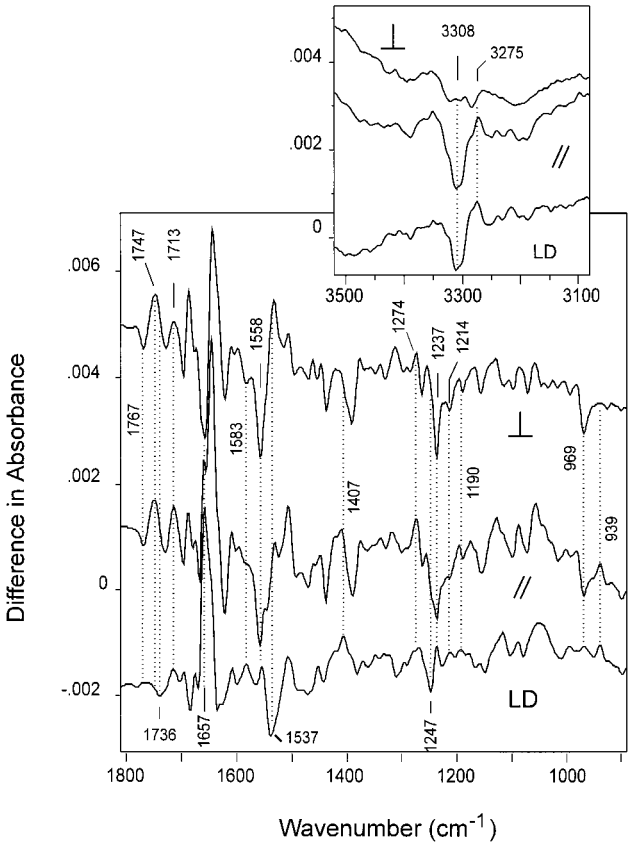

FIGURE 2: Polarized FTIR difference spectroscopy of the rhodopsin to metarhodopsin II transition. Traces shown are the averaged results of 4 samples. LD = || − 1.71 × ⊥. The ⊥-spectrum has been scaled with a factor 1.71 for better comparison. The absorbance scale is for the ||-spectrum. The inset shows the averaged result of two samples in the 3500−3100 cm^{-1} region; the scaling is similar to that in the main panel.

I and amide II bands, respectively. The fraction of unexchanged peptides, f_u, was estimated from $f_u = w_D/w_H$ (*47*). Calculations using different approaches (choice of baseline, peak intensity, peak area etc.) indicate that 60 ± 9% of the peptide groups did not exchange under the experimental conditions, in good agreement with previously reported values (*45*, *47*, *48*).

In contrast to the marked changes observed in the absolute absorption spectra in the H_2O and D_2O condition as a result of H/D exchange, the corresponding LD spectra (Figure 1b) are found to be very similar. Significantly, the relatively intense amide II′ band is found to be essentially nondichroic. Thus, similar to an earlier polarized FTIR study of bacteriorhodopsin (*42*), the combination of polarized light spectroscopy with H/D exchange is able to reveal more information on the structural origin of the exchanging groups of rhodopsin and shows that the latter are located in secondary structures showing little net orientation. Such a differential H/D exchange in rhodopsin was recently also proposed on the basis of unpolarized infrared measurements (*45*) and has also been observed in the early polarized infrared experiments of Michel-Villaz and coauthors (*25*) on oriented intact (frog) rod outer segments.

Orientation of Structural Elements. To calculate the average orientation of the rhodopsin helix bundle with respect to the membrane normal, we used previously determined α values, e.g., the angles of the transition dipole moments (TDMs) relative to the helix long-axis. For example, we used 35° for the amide I band, 75° for the amide II and II′ bands, and 28° for the amide A band (*34*, *36*). The lipid acyl chain orientation was calculated from the dichroism of the methylene ν_s and ν_{as} modes, setting α = 90° (*33*, *36*, *49*). The lipid ester carbonyl band was analyzed using α = 0° (*49*). The results of these calculations are shown in Table 1. The listed dichroic ratios are based on integrated intensities, using baselines calculated between data points. Integrating intervals ranged 3400−3225 cm^{-1} for the amide A band; 2950−2903 cm^{-1}, and 2867−2839 cm^{-1} for the methylene ν_{as} and ν_s bands, 1769−1709 cm^{-1} for the lipid ester C═O band, and 1710−1587 cm^{-1}, 1580−1520 cm^{-1}, and 1500−1390 cm^{-1} for the amide I, amide II, and amide II′ bands, respectively.

First, we note that the lipid acyl chain ordering seems to be slightly higher in the humidified membranes. This might reflect a partial bilayer to H_{II} phase transition in the

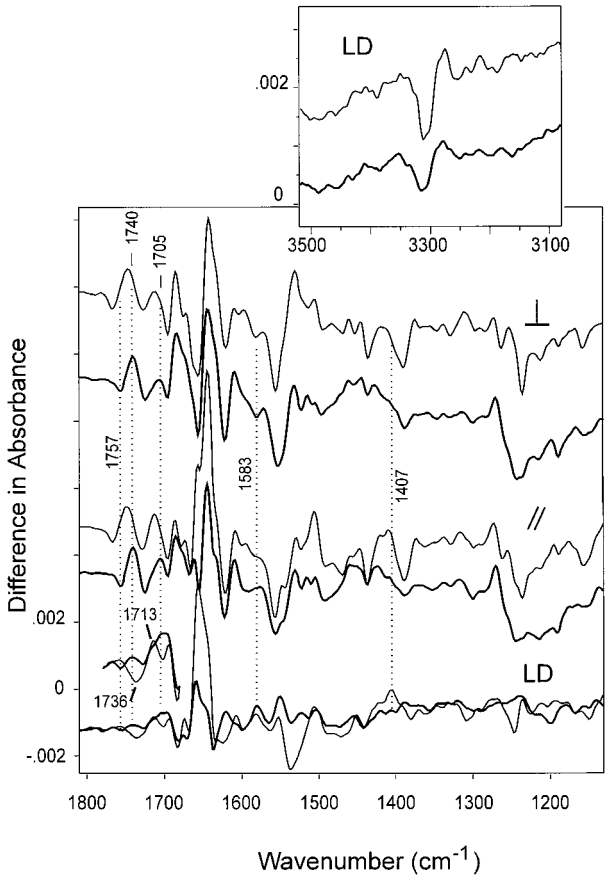

FIGURE 3: Comparison of the FTIR difference spectra of the rhodopsin to metarhodopsin II transition in H_2O or D_2O (thicker lines). LD spectra were calculated using subtraction factors of 1.70 (H_2O) and 1.58 (D_2O), and the corresponding ⊥-spectra were scaled using the same factors. All traces are shown on the same scale; the 1780−1680 cm^{-1} region of the LD spectra has been expanded on the *y*-scale for clarity. The inset shows the LD spectra in the 3500−3100 cm^{-1} region; the scaling is similar to that in the main panel.

Table 1: Values for the Average Dichroic Ratio, *R*, and the Average Angles θ for Selected Vibrational Modes of Oriented Photoreceptor Membrane Films in the Dried ($n = 4$) and Humidified State ($n = 2$)

band	frequency (cm^{-1})	*R*			θ (deg)		
		dried[a]	H_2O[a]	D_2O[a]	dried	H_2O	D_2O
amide A	3289	2.7	nd[c]	3.50	45	nd	38
$\nu_{as}(CH_2)$	2924	1.68	1.52	1.43	47	42	41
$\nu_s(CH_2)$	2853	1.68	1.41	1.34	47	40	38
$\nu_{C=O}$ lipids	1739	1.57	1.26	1.46	60	66	62
amide I	1654	2.24	2.24	2.20	50	50	51
amide II[b]	1545	1.48	1.46	1.32	39	37	32
amide II′	1450	na[c]	na	1.74	na	na	47

[a] Standard deviations were smaller than 7% in *R*, resulting in a smaller than 3° deviation in θ. [b] Variability in these results is 4, 5, and 7° in θ for dried and H_2O/D_2O humidified membranes, respectively, see text. [c] nd, not determined; na, not applicable.

phospholipid membranes upon dehydration, resulting in a decrease in dichroism of the methylene CH_2 stretch bands. The coexistence of these two phases in dried ROS samples has been inferred from X-ray and electron microscopy (*50*, *51*), as well as from ^{31}P NMR studies on ROS membranes (*52*). Second, the average orientation of the rhodopsin helix-bundle in the photoreceptor membrane, obtained from the dichroism of the amide bands in the dried/ and H_2O/D_2O humidified state (45 ± 5/44 ± 7/40 ± 8°) is in good agreement with values of 40 ± 6 and 38° obtained from polarized infrared transmission spectroscopy on dried samples (*26*) and from measurements on intact rod outer segments (*25*), respectively. Third, the orientation calculated from the dichroism of the amide II and amide II′ band in D_2O indeed suggests that the peptide groups which were subject to H/D exchange are located in protein segments exhibiting considerable less net orientation (see above). Having separated the distinct contributions by deuteration, we believe that the best estimate for the overall orientation of rhodopsin should be rather based on the results obtained for the amide A and II bands in D_2O buffer. Hence, we conclude that the average tilt angle of the seven helical segments in rhodopsins membrane domain is at 30−40° with respect to the membrane normal, while the accessible surface regions have a more random distribution.

The above-mentioned qualitative results were found to be only weakly dependent on the choice of the input parameters ($S_{m,f}$, n_3, and α) and the way the spectral parameters were extracted (integrated vs peak intensities, curve-fitting; not shown). In some cases (amide A, amide II) a slight dependence on the choice of the baseline was observed; however, this variability (<7° in $\langle\theta\rangle$) does not affect the general trend of our data. We further note that the internal consistency of the orientations calculated from the amide band dichroisms and the good correspondence to the literature values indicate that the most important assumption in our analysis, i.e., the estimation of the electric-field amplitudes using the two-phase approximation, is indeed valid for both hydrated and dehydrated membranes. Importantly, this gives us a realistic basis to extend our analysis to the case of rhodopsin → metarhodopsin II difference spectra.

Polarized Infrared Difference Spectroscopy. Figure 2 shows the difference spectra of the rhodopsin to metarhodopsin II transition recorded with the IR beam polarized either parallel or perpendicular to the plane of incidence. Since these spectra are calculated by subtracting a rhodopsin spectrum from a metarhodopsin II spectrum, positive bands represent metarhodopsin II and negative bands rhodopsin. These spectra reflect changes of the retinylidene chromophore, which undergoes an 11-cis to all-trans conformational change, as well as structural changes of the protein including those required to expose interaction sites for the G-protein transducin (*7*, *10*, *12*). For example, negative bands at 1558, 1237, 1214, 1190, and 969 cm^{-1} have been assigned to the retinylidene chromophore in rhodopsin upon comparison with resonance Raman (*53*, *54*) and FTIR analyses of rhodopsin analogues containing isotope-labeled chromophores (*10*, *55*). In contrast, few bands have been assigned thus far to specific protein residues except in the 1700−1800 cm^{-1} region (C═O stretch modes of Asp and Glu carboxylic acid groups) (*14*, *16*, *18*, *23*). The LD spectrum has been calculated using a scaling factor of 1.71, and the spectrum recorded with perpendicular polarization has been scaled with the same factor to allow easier visual comparison. The traces shown represent the average of two to four independent experiments, to compensate for slight variations in the baseline. However, we note that the band profiles in the LD spectrum, reflecting the dichroism of the difference bands, was reproducibly observed in every experiment.

Obvious differences between the polarized difference spectra are best observed in the LD spectrum.

The relatively strong LD bands at 1657 (+) and 1537 cm^{-1} (−) can be seen to derive from positive contributions in the parallel and perpendicular polarized spectra, respectively. On this basis, these bands may be assigned to the metarhodopsin II intermediate. The dichroism of this pair qualitatively agrees with the amide I and amide II LD characteristics of α-helical structure, cf. Figure 1, and may thus reflect a small reorientation of helical segment(s) upon activation of rhodopsin. The positive band observed at 3275 cm^{-1}, which lies in the amide A region (assigned to peptide NH stretch vibrations) (*56*) supports this assignment. This band shows significant overlap with a negative band at 3308 cm^{-1}, which is prominently present in the ||-polarized spectrum only, reducing the intensity of the 3275 cm^{-1} band. On the whole, these data suggest a slight reorientation of helical segments in the photoactivation step of rhodopsin, resulting in a smaller angle between the α-helix axis and membrane normal in the metarhodopsin II intermediate.

Bands appearing in the 1700−1800 cm^{-1} region are highly characteristic of C═O stretching modes in esters and protonated carboxylic acid groups in Asp or Glu side chains. By utilizing rhodopsin reconstituted into an ether-phospholipid which lacks the ester carbonyl group, it was shown that contributions from phospholipids in this region of the spectrum are unlikely (*12*). Indeed, the bands observed in the 1780−1710 cm^{-1} range in the rhodopsin to metarhodopsin II difference spectrum have thus far all been tentatively assigned to specific Asp or Glu residues on the basis of mutagenesis data. In this way, the 1767 (−)/1745 (+) and the 1730 (−)/1745 (+) pairs have been assigned to the Asp83 (*14*, *16*) and putatively to the Glu122 (*16*, *18*) COOH group, respectively. Part of the positive band at 1713 cm^{-1} has been assigned to Glu113 (*57*), the counterion to the protonated Schiff base. According to this assignment, Glu113 bears a carboxylate group in rhodopsin and the corresponding vibrations have been tentatively assigned to bands at 1590 and 1395 cm^{-1} (*57*).

Interestingly, the major band observed in this region of the LD spectrum is at 1736 cm^{-1} (−), at a position where a specific band has yet not been detected in the unpolarized difference spectrum of the rhodopsin → metarhodopsin II transition. Furthermore, this LD band is sensitive to H/D exchange as discussed below and is therefore assigned to a protein carboxyl group. Only much smaller LD bands are observed at the position of the Asp83 bands (1767/1745 cm^{-1}), indicating that this group is not strongly immobilized or is located near the magic angle (54.6°) where the dichroism is 0. Two strongly dichroic bands are also observed at 1407 and 1583 cm^{-1}, in the frequency ranges expected for the symmetric and asymmetric stretching vibrations of a carboxylate group. Combination of the latter two bands with the band at 1736 cm^{-1} could represent either the deprotonation or the protonation of a previously undetected Asp or Glu residue.

A moderately strong LD band is also observed at 1247 cm^{-1} (−). In a previous paper, the role of tyrosines in the rhodopsin to metarhodopsin II transition has been specifically addressed using stable-isotope (ring-deuterated tyrosine) labeling (*24*). Among other things, it was found that there is a negative band at 1248 cm^{-1} assignable to the bending vibration of a tyrosine hydroxyl function in rhodopsin. The 1247 cm^{-1} LD band observed in the present study could therefore represent a reorientation of this tyrosine side-chain upon photoexcitation. We are presently in the process of incorporating single-^{13}C-labeled tyrosine into rhodopsin; this should facilitate definite assignment of tyrosine vibrations to specific tyrosine modes.

The difference spectrum taken with parallel polarization further shows an additional band at 939 cm^{-1}, which lies within a region characteristic of hydrogen-out-of-plane (HOOP) wag modes. In previous FTIR studies (*55*), using rhodopsin analogues containing a stable-isotope labeled chromophore, bands at 947 and 950 cm^{-1} have been identified to derive from the retinal HC_{11}═$C_{12}H$ A_u HOOP combination in lumirhodopsin and metarhodopsin I, respectively. In metarhodopsin II, a band assignable to this mode has never been reported. This vibration is the best candidate for the 939 cm^{-1} (+) band of metarhodopsin II. The presence of this band only in the spectrum taken with parallel polarization would then indicate a significant change in orientation of the HC_{11}═$C_{12}H$ group during the final activation step of rhodopsin. A definitive assignment, however, requires the use of selectively labeled chromophores, and this work is in progress.

In Figure 3, the polarized difference spectra recorded in H_2O are compared to those obtained in D_2O buffer. As in the case of the absolute absorbance spectra, the difference spectra also exhibit characteristic isotope induced band shifts (*16*, *17*). Overall, the net intensity of the LD spectrum in D_2O is significantly smaller than that in H_2O. For example, the bands in the amide A, I, and II regions [3275 (+), 1657 (+) and 1537 cm^{-1} (−), respectively] are reduced in intensity. Assuming the above assignment of these bands to amide modes is correct, the H/D sensitivity of the amide A and II bands indicates that the involved helical structures are positioned in a region accessible to H/D exchange, implying a localization near the membrane surface. The loss of intensity in the amide I region, however, is somewhat puzzling. Clearly, the reduced sensitivity to the polarization of the IR probe beam cannot be ascribed to a reduced net orientation of the samples (cf. Table 1). Indeed, the orientation obtained from the bands assigned to D83 in D_2O was found to be the same as in H_2O (see below). On the other hand, additional H/D exchange triggered by bleaching, extensively discussed in a previous paper (*45*), produces additional difference bands near 1660/1632 cm^{-1}. Therefore, we currently believe that the reduced 1657 cm^{-1} LD contribution in D_2O is rather caused by mixing with downshifted, nonhelical, amide I contributions.

The dichroic difference spectra in Figure 3 further indicate that the 1736 (−) band shifts down to ± 1720 cm^{-1} in D_2O, effectively canceling the positive, H/D insensitive part of the peak at 1713 cm^{-1}. The H/D sensitive part of the band at 1713 cm^{-1}, assigned to E113, shifts down to 1705 cm^{-1}, in agreement with earlier studies (*57*). Notably, the 1407 and 1583 cm^{-1} bands are still present in the D_2O data, whereas the 1736 cm^{-1} band clearly shows an isotope induced shift, in general agreement with the assignment discussed above.

Intramolecular Orientations from Polarized Difference Spectroscopy. Table 2 shows the apparent orientations calculated from the dichroism of selected bands in the H_2O data set, taking $\alpha = 0°$, which assumes that the TDM runs

Table 2: Dichroic Ratio, R, and Orientation Angle θ, for Selected Absorption Bands in the Rhodopsin (rho) to Metarhodopsin II (MII) Transition in H_2O Buffer ($n = 4$, except for the 3308 cm^{-1} Band: $n = 2$)[a]

frequency (cm^{-1})	assignment	R	θ (deg)[b]
3308 (−)	?	6.5	33
1768 (−)	D83 side chain C═O in rho[c]	1.50	61
1748 (+)	D83 side chain C═O in MII[c]	2.0	55
1713 (+)	E113 side chain C═O in MII[d]	2.68	49
1687 (+)	?	0.83	82
1621 (−)	?	2.0	55
1558 (−)	retinal C═C stretch mode in rho[e]	1.9	56
1274 (+)	Tyrosinate C−O^- stretch in MII[f]	2.3	52
1237 (−)	retinal C_{12}−C_{13} stretch in rho[e]	0.96	75
1214 (−)	retinal C_8−C_9 stretch in rho[e]	1.12	70
1190 (−)	retinal C_{14}−C_{15} stretch in rho[e]	1.4	63
969 (−)	retinal HC_{11}═$C_{12}H$ HOOP in rho[g]	1.39	63
939 (+)	retinal HC_{11}═$C_{12}H$ HOOP in MII	6.8	32

[a] All analyses were performed using $\alpha = 0$. [b] Standard deviations were smaller than 3°, except for the 1748 cm^{-1} band (7°). [c] Assignment based on Rath et al. and Fahmy et al. (*14*, *16*). [d] Assignment based on Jäger et al. (*57*). [e] Assignment based on Palings et al. (*53*). [f] Assignment based on DeLange et al. (*24*). [g] Assignment based on Palings et al. (*54*).

parallel to the atomic bond (see Discussion). Integrating intervals were chosen such that only one dichroic difference band (LD) was located in that region. Since the bands in the 1630−1680 and 1550−1490 cm^{-1} regions are prone to lead to erroneous results due to extreme overlap, they were not taken into account. For similar reasons, we were not able to determine the dichroic ratio of the 1736 and 1583 cm^{-1} bands. The dichroic ratio of the 1407 cm^{-1} band was found to be 4.8 ± 0.1, from which we calculated that its transition moment lies at 38° with respect to the membrane normal.

As an additional check on sample orientation in D_2O, assuming that the coupling effects of the O−H bending mode to the orientation of the C═O TDM are negligible (*58*), orientations were calculated from the dichroism of the 1757 (−)/1740 (+) pair, assigned to Asp83. Orientations of 56° (1757 cm^{-1} band) and 57° (1740 cm^{-1}) were obtained for the D83 side chain C═O band in rhodopsin and metarhodopsin II, respectively, i.e., essentially identical to those obtained from the data in H_2O.

DISCUSSION

In this paper, we report the first application of polarized ATR-FTIR difference spectroscopy to investigate the orientation of individual groups in bovine rhodopsin. Previously, only the macroscopic orientation of rhodopsin in its native membrane has been investigated using polarized transmission FTIR spectroscopy (*26*). In the case of bacteriorhodopsin, infrared linear dichroism studies, in combination with difference spectroscopy, already provided detailed information on intramolecular orientations including the orientation of the retinylidene polyene plane relative to the membrane plane and specific protein groups (*58*−*62*).

In infrared LD measurements based on transmission spectroscopy, a tilt angle series is normally conducted where the sample plane is tilted with respect to the direction of incident radiation. (*26*, *60*, *63*). Extensive data acquisition and averaging is often necessary in these experiments since the dichroism tends to be small at low angles. However, for analysis of rhodopsin to metarhodopsin II difference spectra, which are essentially obtained from a single photolytic reaction, a tilt series analysis is not readily accomplished on the same sample. This problem does not exist in the ATR mode, where both polarization angles can be alternately monitored. The ATR technique offers the additional advantage over transmission spectroscopy that the sample is probed with the maximal difference in polarization of 90° with respect to the sample plane, whereas in transmission mode the maximal tilt angle usually is about 60°. This is an important advantage since it significantly increases the sensitivity of the measurements.

Macroscopic Orientation and H/D Exchange. The macroscopic orientation of rhodopsin in its native disk membrane was determined and compared to literature data in order to check on the validity of the method of analysis. The membranes were studied in both the dried and humidified state (H_2O and D_2O). The present estimate of 45 ± 5° (Table 1) for the average orientation of rhodopsins helix bundle is in good agreement with the previously reported value from polarized transmission experiments on (dried) oriented samples (*26*).

When combined with hydrogen−deuterium exchange, polarized absorbance spectra can also provide information on the regions of the protein most accessible to the aqueous phase. It is found that the inaccessible helical core of the protein has an average orientation of 30−40° with respect to the membrane normal, while the more accessible parts have a more random distribution. These results substantiate the predictions based on previously reported unpolarized infrared studies (*45*).

Polarized IR Difference Spectroscopy. The rhodopsin to metarhodopsin II difference spectra obtained with the polarization of the IR light perpendicular to the plane of incidence most closely resemble the unpolarized transmission mode difference spectra previously reported from our laboratories (*12*, *14*, *17*, *18*, *24*, *64*). This is not unexpected, since, in transmission experiments the polarization of the incident light will be in the plane of the membrane for the well-oriented samples we routinely use. The photoreceptor membrane samples we use for transmission FTIR are routinely prepared by spin-drying a photoreceptor membrane suspension onto an IR transparent substrate, which yields well-oriented membrane films (*65*−*67*). On the other hand, the parallel polarized difference spectrum is obtained using a polarization direction that should not be present in transmission measurements on oriented samples. Indeed, these difference spectra exhibit several new bands such as the one at 939 cm^{-1}, which we tentatively assign to the HC_{11}═$C_{12}H$ hydrogen-out-of-plane (HOOP) mode of the all-trans retinylidene chromophore in metarhodopsin II.

Orientation of the Chromophore. The present work yields information on the relative orientation of specific groups in the retinylidene chromophore. The data in Table 2 show that the C═C and C−C TDMs for the chromophore polyene chain in rhodopsin have tilt angles in the range 56−75°, in qualitative agreement with visible LD studies, indicating that the electronic dipole moment of the 498 nm transition, oriented approximately along a vector connecting the Schiff base nitrogen and the ionone-ring portion, lies at 16° with respect to the membrane plane (*27*). It should be noted, however, that obtaining global chromophore orientations from individual chromophore bands relies on accurate

knowledge on the orientation of the infrared dipole moment (which may be the sum of various contributing normal modes) relative to the retinal plane. Mixing of normal modes may cause the net vibrational TDM of the band to deviate from the C−C or C═C bond directors, i.e., α may not be 0° (*58, 60*−*62*). Furthermore, the retinal moiety in rhodopsin adopts a skewed 11-cis conformation and exhibits considerable twists around the carbon−carbon bonds in the isomerization region (C_{10}···C_{13}) (*68, 69*). Due to these twists, the HOOP modes may mix with in-plane modes (e.g., C═C and C−C stretch and C−CH bending modes) by which they loose their pure out-of-plane character (*58, 61, 62*). More quantitative analyses of the retinal conformation therefore must await further theoretical (normal-mode) and experimental efforts.

It has been suggested from visible dichroism studies (*28*) that the chromophore in metarhodopsin II transiently adopts a more in (membrane) plane orientation of 5 ± 4°. However, we could not address such overall effects, since, apart from the newly assigned band at 939 cm^{-1}, few bands have been identified to derive from the all-trans chromophore in metarhodopsin II. Using ^{13}C labeled retinals, we are currently trying to identify these bands which should facilitate orientation studies of the chromophore in this late phase of the photocascade.

The discovery of a new band in the rhodopsin to metarhodopsin II difference spectrum deserves special mention. The intensity of the 939 cm^{-1} (+) band is significantly lower than that of the HOOP bands in lumirhodopsin and metarhodopsin I, where it is approximately as intense as the 969 cm^{-1} (−) rhodopsin band. This may be due to the more relaxed local structure or to secondary effects caused by the deprotonation of the Schiff base linkage in the metarhodopsin I to metarhodopsin II transition (*55*). In any case, if the assignment of this band to an A_u-HOOP mode proves to be correct, the fact that in metarhodopsin I this mode strongly responds to perpendicular polarized light (i.e., obvious in "unpolarized" FTIR difference spectra of oriented membrane films), but in metarhodopsin II only to parallel polarized light, indicates that the HC_{11}═$C_{12}H$ group significantly reorients during this transition. Possibly, this represents a second essential conformational change in the chromophore, permitting proton transfer from the Schiff base, and finally leads to the rearrangements in the protein necessary to expose its signaling sites. This would agree with the observation that an additional methyl group at the 10-position of the retinal strongly retards the metarhodopsin I to metarhodopsin II transition (*64*).

Intramolecular (re-)Orientation of Protein Groups during Photoactivation. The highest sensitivity to the direction of polarization in the rhodopsin to metarhodopsin II transition was observed in the amide regions. In the linear dichroic difference spectrum, the amide I contribution is strongly positive whereas that in the amide II region is negative. The polarized difference spectra indicate that these bands stem from the metarhodopsin II intermediate. A corresponding positive amide A band may be located at 3275 cm^{-1}, although this band seems to be largely obscured by a strong band at 3308 cm^{-1}, possibly due to a peptide NH stretch mode. The overall appearance of these bands in the dichroic difference spectra is strikingly similar to those characteristic of oriented helical structures (cf. the absolute spectra in Figure 1). Hence, the most direct interpretation is that these bands reflect a small reorientation of helical structure, and the pattern observed is consistent with the net tilting of α-helical structures toward the membrane normal during the rhodopsin to metarhodopsin II transition. In a previous paper (*24*), we discussed that the fully conserved Pro/Tyr pair in helix 6 in all visual pigments may be acting as a hinge for movements in this helix in response to chromophore isomerization. Possibly in relation to this, the present work provides evidence for a tyrosine mode (1247 cm^{-1}) which changes its orientation in the rhodopsin to metarhodopsin II transition. Overall, this agrees with and complements previous results, obtained from electron paramagnetic resonance spectroscopy on site-directed spin-labeled rhodopsin, which were interpreted to reflect rigid body movement involving parts of helix 3 and/or 6, resulting in a more expanded structure of the cytoplasmic side of rhodopsin in the activation step (*70*).

FTIR difference spectroscopy has been especially successful in identifying changes in the hydrogen-bonding environment and protonation state of residues carrying carboxylic acid groups (e.g., Asp83, Glu113, and Glu122; see Results). The highly conserved Glu134 has been associated with light-dependent proton uptake and signaling in rhodopsin (*31*) and, therefore, is also expected to become protonated in the activation step. However, to date, bands assignable to this protonation reaction could not be identified from FTIR studies on E134 mutants (*16, 18*). We now suggest that the strong bands observed in the dichroic difference spectrum at 1736 (carboxyl), 1583, and 1407 cm^{-1} (carboxylate asymmetric and symmetric stretch, respectively) may represent the protonation of E134 in the rhodopsin to metarhodopsin II transition.[2] It would also follow that this group has restricted mobility and is oriented toward the plane of the membrane. In unpolarized difference spectra this band is probably obscured by the other strong carboxyl bands. Although definite assignment will require further studies involving site-directed mutagenesis, additional support comes from a recent study describing ATR-FTIR studies on complex formation between bovine rhodopsin and transducin and transducin derived peptides (*71*). A band at 1735 cm^{-1} was clearly observed in the double difference spectrum representing the rhodopsin to metarhodopsin II transition in the absence or presence of transducin and was tentatively assigned to protonation of Glu134 induced by transducin binding. The protonation of Glu134 does not depend, however, on the presence of transducin (*31*), and we rather propose that the band observable upon complex formation with transducin may reflect a reorientation of the carboxyl group of Glu134 protonated at an earlier stage, rather than the protonation of this residue.

Conclusion. In this work, we demonstrate the potential of polarized ATR-FTIR difference spectroscopy to obtain highly detailed information on intramolecular orientations in rhodopsin. Evidence is presented for a small reorientation of helical segments in the activation of rhodopsin as well as for the protonation of a previously undetected carboxyl-group-bearing residue. Additionally, the dichroic properties of the bands in the HOOP region suggest a localized reorientation in the retinal polyene tail in the late phase of photoactivation.

[2] These bands may have escaped detection in the difference spectra of mutants E134D and E134R because of the severe overlap in these regions (*18*).

Significantly, the use of polarized probe light yields additional resolving power and facilitates the analysis of component bands in spectral regions showing considerable overlap. Future perspectives include studies on oriented membranes of rhodopsin analogues and recombinant rhodopsin, which are in progress. In combination with site-directed mutagenesis and (site-directed) isotope labeling, this will allow both identification as well as orientation studies of additional protein groups involved in activation of rhodopsin.

ACKNOWLEDGMENT

We thank Dr. E. Goormaghtigh for helpful discussions.

REFERENCES

1. Baldwin, J. M., Schertler, G. F. X., and Unger, V. M. (1997) *J. Mol. Biol. 272*, 144−164.
2. Schoenlein, R. W., Peteanu, L. A., Mathies, R. A., and Shank, C. V. (1991) *Science 254*, 412−415.
3. Yoshizawa, T., and Wald, G. (1963) *Nature 197*, 1279−1286.
4. Wald, G. (1968) *Science 162*, 230−239.
5. Emeis, D., Kühn, H., Reichert, J., and Hofmann, K. P. (1982) *FEBS Lett. 143*, 29−34.
6. Kibelbek, J., Mitchell, D. C., Beach, J. M., and Litman, B. J. (1991) *Biochemistry 30*, 6761−6768.
7. Rothschild, K. J., Cantore, W. A., and Marrero, H. (1983) *Science 219*, 1333−1335.
8. Rothschild, K. J., Gillespie, J., and DeGrip, W. J. (1987) *Biophys. J. 51*, 345−350.
9. Siebert, F., Maentele, W., and Gerwert, K. (1983) *Eur. J. Biochem. 136*, 119−127.
10. Bagley, K. A., Balogh-Nair, V., Croteau, A. A., Dollinger, G., Ebrey, T. G., Eisenstein, L., Hong, M. K., Nakanishi, K., and Vittitow, J. (1985) *Biochemistry 24*, 6055−6071.
11. Rothschild, K. J., and DeGrip, W. J. (1986) *Photobiochem. Photobiophys. 13*, 245−258.
12. DeGrip, W. J., Gray, D., Gillespie, J., Bovee, P. H. M., Van den Berg, E. M. M., Lugtenburg, J., and Rothschild, K. J. (1988) *Photochem. Photobiol. 48*, 497−504.
13. Klinger, A. L., and Braiman, M. S. (1992) *Biophys. J. 63*, 1244−1255.
14. Rath, P., DeCaluwé, G. L. J., Bovee-Geurts, P. H. M., DeGrip, W. J., and Rothschild, K. J. (1993) *Biochemistry 32*, 10277−10282.
15. Maeda, A., Ohkita, Y. J., Sasaki, J., Shichida, Y., and Yoshizawa, T. (1993) *Biochemistry 32*, 12033−12038.
16. Fahmy, K., Jäger, F., Beck, M., Zvyaga, T., Sakmar, T. P., and Siebert, F. (1993) *Proc. Natl. Acad. Sci. U.S.A. 90*, 10206−10210.
17. Rath, P., Bovee-Geurts, P. H. M., DeGrip, W. J., and Rothschild, K. J. (1994) *Biophys. J. 66*, 2085−2091.
18. DeCaluwé, G. L. J., Bovee-Geurts, P. H. M., Rath, P., Rothschild, K. J., and DeGrip, W. J. (1995) *Biophys. Chem. 56*, 79−87.
19. Kandori, H., and Maeda, A. (1995) *Biochemistry 34*, 14220−14229.
20. Nishimura, S., Sasaki, J., Kandori, H., Matsuda, T., Fukada, Y., and Maeda, A. (1996) *Biochemistry 35*, 13267−13271.
21. Nishimura, S., Kandori, H., and Maeda, A. (1997) *Photochem. Photobiol. 66*, 796−801.
22. Rath, P., DeLange, F., DeGrip, W. J., and Rothschild, K. J. (1998) *Biochem. J. 329*, 713−717.
23. Beck, M., Sakmar, T. P., and Siebert, F. (1998) *Biochemistry 37*, 7630−7639.
24. DeLange, F., Klaassen, C. H. W., Bovee-Geurts, P. H M., Wallace-Williams, S. E., Liu, X.-M., DeGrip W. J., and Rothschild, K. J. (1998) *J. Biol. Chem. 273*, 23735−23739.
25. Michel-Villaz, M., Saibil, H. R., and Chabre, M. (1979) *Proc. Natl. Acad. Sci. U.S.A. 76*, 4405−4408.
26. Rothschild, K. J., Sanches, R., Hsiao, T. L., and Clark, N. A. (1980) *Biophys. J. 31*, 53−64.
27. Liebman, P. A. (1962) *Biophys. J. 2*, 161−178.
28. Chabre, M., and Breton, J. (1979) *Vision Res. 19*, 1005−1018.
29. Lewis, J. W., Einterz, C. M., Hug, S. J., and Kliger, J. S. (1989) *Biophys. J. 56*, 1101−1111.
30. Gröbner, G., Choi, G., Burnett, I. J., Glaubitz, C., Verdegem, P. J. E., Lugtenburg, J., and Watts, A. (1998) *FEBS Lett. 422*, 201−204.
31. Arnis, S., Fahmy, K., Hofmann, K. P., and Sakmar, T. P. (1994) *J. Biol. Chem. 269*, 23879−23881.
32. DeGrip, W. J., Daemen, F. J. M., and Bonting, S. L. (1980) *Methods Enzymol. 67*, 301−320.
33. Fringeli, U. P., and Guenthard, Hs. H (1981) in *Membrane Spectroscopy* (Grell, E., Ed.) Vol. 31, pp 270−332, Springer-Verlag, New York.
34. Ludlam, C. F. C., Arkin, I. T., Liu, X.-M., Rothman, M. S., Rath, P., Aimoto, S., Smith, S. O., Engelman, D. M., and Rothschild, K. J. (1996) *Biophys. J. 70*, 1728−1736.
35. Harrick, N. J. (1967) *Internal Reflection Spectroscopy*, Interscience Publishers, New York.
36. Frey, S., and Tamm, L. K. (1991) *Biophys. J. 60*, 922−930.
37. Arkin, I. T., Rothman, M., Ludlam, C. F. C., Aimoto, S., Engelman, D. M., Rothschild, K. J., and Smith, S. O. (1995) *J. Mol. Biol. 248*, 824−834.
38. Fraser, R. D. B., and MacRae, T. P. (1973) *Conformation in Fibrous Proteins and Related Synthetic Polypeptides*, pp 179−217, Academic Press, New York.
39. Harrick, N. J. (1965) *J. Opt. Soc. Am. 55*, 851−857.
40. Pistorius, A. M. A., and DeGrip, W. J. (1994) *Biochem. Biophys. Res. Commun. 198*, 1040−1045.
41. Nabedryk, E., Andrianambinintsoa, S., and Breton, J. (1984) *Biochim. Biophys. Acta 765*, 380−387.
42. Earnest, T. N., Herzfeld, J., and Rothschild, K. J. (1990) *Biophys. J. 58*, 1539−1546.
43. Goormaghtigh, E., and Ruysschaert, J.-M (1989) in *Molecular Description of Biological Membranes by Computer Aided Conformational Analysis* (Brasseur, R., Ed.) Vol. 1, pp 285−330, CRC Press, Boca Raton.
44. Hunt, J. F., Earnest, T. N., Bousche, O., Kalghatgi, K., Reilly, K., Horvath, C., Rothschild, K. J., and Engelman, D. M. (1997) *Biochemistry 36*, 15156−15176.
45. Rath, P., DeGrip, W. J., and Rothschild, K. J. (1998) *Biophys. J. 74*, 192−198.
46. Miyazawa, T., Shimanouchi, T., and Mizushima, S. (1958) *J. Chem. Phys. 29*, 611−616.
47. Downer, N. W., Bruchman, T. J., and Hazzard, J. H. (1986) *J. Biol. Chem. 261*, 3640−3647.
48. Haris, P. I., Coke, M., and Chapman, D. (1989) *Biochim. Biophys. Acta 995*, 160−167.
49. Nabet, A., Boggs, J. M., and Pézolet, M. (1994) *Biochemistry 33*, 14792−14799.
50. Gruner, S. M., Rothschild, K. J., and Clark, N. A. (1982) *Biophys. J. 39*, 241−251.
51. Gruner, S. M., Rothschild, K. J., DeGrip, W. J., and Clark, N. A. (1985) *J. Phys. 46*, 193−201.
52. Gröbner, G., Taylor, A., Williamson, P. T. F., Choi, G., Glaubitz, C., Watts, J. A., DeGrip, W. J., and Watts, A. (1997) *Anal. Biochem. 254*, 132−138.
53. Palings, I., Pardoen, J. A., van den Berg, E. M. M., Winkel, C., Lugtenburg, J., and Mathies, R. A. (1987) *Biochemistry 26*, 2544−2556.
54. Palings, I., van den Berg, E. M. M., Lugtenburg, J., and Mathies, R. A. (1989) *Biochemistry 28*, 1498−1507.
55. Ohkita, Y. J., Sasaki, J., Maeda, A., Yoshizawa, T., Groesbeek, M., Verdegem, P., and Lugtenburg, J. (1995) *Biophys. Chem. 56*, 71−78.
56. Parker, F. S. (1983) *Applications of infrared, Raman and resonance Raman spectroscopy in biochemistry*, Plenum Press, New York.
57. Jäger, F., Fahmy, K., Sakmar, T. P., and Siebert, F. (1994) *Biochemistry 33*, 10878−10882.
58. Fahmy, K., Siebert, F., and Tavan, P. (1991) *Biophys. J. 60*, 989−1001.

59. Nabedryk, E., and Breton, J. (1986) *FEBS Lett. 202*, 356−360.
60. Earnest, T. N., Roepe, P., Braiman, M. S., Gillespie, J., and Rothschild, K. J. (1986) *Biochemistry 25*, 7793−7798.
61. Fahmy, K., Siebert, F., Grossjean, M. F., and Tavan, P. (1989) *J. Mol. Struct. 214*, 257−288.
62. Breton, J., and Nabedryk, E. (1989) *Biochim. Biophys. Acta 973*, 13−18.
63. Rothschild, K. J., and Clark, N. A. (1979) *Biophys. J. 25*, 473−488.
64. DeLange, F., Bovee-Geurts, P. H. M., VanOostrum, J., Portier, M. D., Verdegem, P. J. E., Lugtenburg, J., and DeGrip, W. J. (1998) *Biochemistry 37*, 1411−1420.
65. Clark, N. A., Rothschild, K. J., Luippold, D. A., and Simon, A. (1980) *Biophys. J. 31*, 65−96.
66. Rothschild, K. J., Sanches, R., Hsiao, T. L., and Clark, N. A. (1980) *Biophys. J. 31*, 53−64.
67. Rothschild, K. J., Rosen, K. M., and Clark, N. A (1980) *Biophys. J. 31*, 45−52.
68. Feng, X., Verdegem, P. J. E., Lee, Y. K., Sandstroem, D., Eden, E., Bovee-Geurts, P., DeGrip, W. J., Lugtenburg, J., de Groot, H. J. M., and Levitt, M. H. (1997) *J. Am. Chem. Soc. 119*, 6853−6857.
69. Bifone, A., DeGroot, H. J. M., and Buda, F. (1997) *J. Phys. Chem. B 101*, 2954−2958.
70. Farrens, D. L., Altenbach, C., Yang, K., Hubbell, W. L., and Khorana, H. G. (1996) *Science 274*, 768−770.
71. Fahmy, K. (1998) *Biophys. J. 75*, 1306−1318.

BI9909501